PHYSICAL REVIEW B **70**, 134428 (2004)

Magnetocaloric effect in the $R\mathrm{Ni}_5$ (R=Pr, Nd, Gd, Tb, Dy, Ho, Er) series

P. J. von Ranke,[1,*] M. A. Mota,[2] D. F. Grangeia,[1] A. Magnus G. Carvalho,[2] F. C. G. Gandra,[2] A. A. Coelho,[2] A. Caldas,[3] N. A. de Oliveira,[1] and S. Gama[2]

[1]*Instituto de Física, Universidade do Estado do Rio de Janeiro, Rua São Francisco Xavier, 524, 20550-013, RJ, Brazil*

[2]*Instituto de Física 'Gleb Wataghin', Universidade Estadual de Campinas-UNICAMP, C.P. 6165, Campinas 13 083-970, SP, Brazil*

[3]*Universidade Gama Filho, Rua Manoel Vitorino, 625, 20740-280, Piedade, Rio de Janeiro, RJ, Brazil*

(Received 17 April 2004; published 29 October 2004)

In this paper, the magnetocaloric effect in the hexagonal intermetallic compounds belonging to the $R\mathrm{Ni}_5$ series was calculated using a Hamiltonian including the crystalline electrical field, exchange interaction, and the Zeeman effect. Experimental work was performed and the two thermodynamics quantities, namely, isothermal entropy change and adiabatic temperature change were obtained for polycrystalline samples, using heat capacity measurements, and compared to the theoretical predictions.

DOI: 10.1103/PhysRevB.70.134428 PACS number(s): 75.30.Sg, 75.40.Cx, 74.25.Ha, 65.40.−b

INTRODUCTION

Many magnetic materials studied in the past have been experimentally and theoretically reinvestigated focusing on the magnetocaloric effect (MCE), i.e., the ability of magnetic materials to heat up when they are magnetized, and cool down when removed from the magnetic field. The recent renewed interest in the MCE appears after the discovery of the giant magnetocaloric effect in $Gd_5(Si_2Ge_2)$ near room temperature.[1] The magnetocaloric materials present great technological interest in the refrigeration field since magnetic refrigeration gives one of the most efficient and ecological methods of cooling around room temperature and even higher.[2] More recently, two other potential magnetocaloric materials, namely $MnFeP_{0.45}As_{0.55}$ (Ref. 3) and $MnAs_{1-x}Sb_x$,[4,5] were reported with giant magnetocaloric effect around room temperature. In the three above-mentioned materials the first order magnetic phase transition from ferromagnetic to paramagnetic state is present and associated to the experimental observation of the giant-magnetocaloric effect. Theoretical investigations on these materials were recently reported in Refs. 6, 7, and 8.

Besides the technological interest, it is important to understand the MCE in terms of fundamental physics. For example, the giant quadrupolar interaction present in the YbAs compound[9] and the quantum crossing effect in $PrNi_5$ (Ref. 10) were well described by analyzing the isothermal entropy change, ΔS_{mag}, that occur upon change of an applied magnetic field using the appropriate Hamiltonian. The entropic investigation (i.e., ΔS_{mag} vs temperature) showed that the magnetic entropy in $PrNi_5$ (which is a paramagnetic compound) increases with the application of magnetic field at low temperature, the so-called anomalous entropy variation effect.

Motivated by the anomalous entropy effect observed in $PrNi_5$, in this paper we fully investigated the MCE in the $R\mathrm{Ni}_5$ series (R=rare-earth element). The MCE, which is characterized by the two thermodynamic quantities, namely, ΔS_{mag} (mentioned above) and the adiabatic temperature change, ΔT_{ad}, were theoretically calculated and experimentally measured in this series by heat capacity measurements in 0 and 5 teslas. Here we report on the results of this work.

THEORY

The $R\mathrm{Ni}_5$ compounds crystallize in the hexagonal $CaCu_5$-type structure[11] and its magnetism is due to the R^{3+} ions. Therefore, the simplest theoretical approximation to model the localized magnetic properties of $R\mathrm{Ni}_5$ compounds is given by the following Hamiltonian:

$$\hat{H} = \hat{H}_{\mathrm{CEF}} + \hat{H}_{\mathrm{MAG}}, \tag{1}$$

where

$$\hat{H}_{\mathrm{CEF}} = B_2^0 O_2^0 + B_4^0 O_4^0 + B_6^0 O_6^0 + B_6^6 O_6^6 \tag{2}$$

and

$$\hat{H}_{\mathrm{MAG}} = -g\mu_B H[\cos(\alpha)J^x + \cos(\beta)J^y + \cos(\gamma)J^z], \tag{3}$$

Relation (2) gives the single ion crystal electrical field (CEF) Hamiltonian, where O_n^m are the Steven's equivalent operators,[12] and the coefficients, B_n^m, determine the strength of the splitting of the $(2J+1)$-fold degenerate Hund ground multiplet, with J the total angular momentum. Relation (3) is the single ion magnetic Hamiltonian, taken in the molecular field approximation, where g is the Landè factor, μ_B is the Bohr magneton and $H=H_0+\lambda M$ is the effective exchange field (external magnetic field plus the effective molecular field) with the molecular field constant λ, and $M=g\mu_B\langle\cos(\alpha)J^x+\cos(\beta)J^y+\cos(\gamma)J^z\rangle$ being the magnetization in the easy magnetic direction. The symbols J^η, $\eta=x, y, z$ stand for the three components of the total angular momentum operator with the direction cosines relative to the crystallographic axis.

The magnetic state equation is obtained by taking the Boltzmann mean value of the magnetic dipole operator,

TABLE I. Magnetic parameters for intermetallics compounds belonging to $R\mathrm{Ni}_5$ series.

Compounds	B_2^0	$B_4^0\times 10^2$	$B_6^0\times 10^4$	$B_6^6\times 10^2$	λ	T_c	Easy direction	Reference
$GdNi_5$						32		15
$DyNi_5$	0.198	0.0190	0.0095	0.0024		11.6	*b*	16
$HoNi_5$	0.0991	0.0164	−0.0017	−0.0026	3.09	5	*a*	17
$NdNi_5$	0.289	0.125	−0.302	−0.116	63.77	8	*a*	18
$TbNi_5$	0.331	−0.0034	−0.0345	−0.0034	13.88	23	*a*	19
$ErNi_5$	−0.0732	−0.0092	0.0124	0.0028		9	*c*	20
$PrNi_5$	0.61	0.496	1.01	0.27	29.84		*a*	21

$$M = g\mu_B\langle J^\eta\rangle = g\mu_B \frac{\sum \langle\varepsilon_i|J^\eta|\varepsilon_i\rangle \exp\left(-\frac{\varepsilon_i}{KT}\right)}{\sum \exp\left(-\frac{\varepsilon_i}{KT}\right)}. \quad (4)$$

The ε_i and $|\varepsilon_i\rangle$ are the energy eigenvalues and eigenvectors, respectively, of Hamiltonian (1) and J^η is the component of the total angular momentum at an arbitrary direction η. The magnetization and the magnetic entropy are determined under the self-consistent solution of Eqs. (4).

The magnetic entropy can be determined by the general relation, obtained from Helmholtz free energy,

$$S_M(T,H_0) = \left(\frac{1}{T}\right)\frac{\sum_{k=1}^{2J+1} \varepsilon_k \exp(-\varepsilon_k/k_BT)}{\sum_{k=1}^{2J+1} \exp(-\varepsilon_k/k_BT)} + k_B \ln\left[\sum_{k=1}^{2J+1} \exp(-\varepsilon_k/k_BT)\right], \quad (5)$$

where k_B is the Boltzman constant. The lattice entropy can be calculated by the Debye formula,

$$S_{\mathrm{latt}} = -3nR\ln[1-\exp(-T_D/T)] + 12nR\left(\frac{T}{T_D}\right)^3 \int_0^{T_D/T} \frac{x^3\,dx}{\exp(x)-1}, \quad (6)$$

where R is the gas constant and T_D is the Debye temperature. The electronic entropy is given by $S_{\mathrm{ele}}=\overline{\gamma}T$ where the Sommerfeld coefficient $\overline{\gamma}=36$ mJ/mol K^2, is taken from the nonmagnetic reference compound $LaNi_5$,[13] and is assumed to be the same for the whole series. The total entropy at any temperature and magnetic field is given by $S_T=S_{\mathrm{mag}}+S_{\mathrm{latt}}+S_{\mathrm{ele}}$.

After the above entropy calculations, the isothermal total entropy changes, ΔS_T, that occurs for changes in the external magnetic field, can be directly determined,

$$\Delta S_T(T,\Delta H) = S_T(T,H_2) - S_T(T,H_1). \quad (7)$$

If the magnetic field and the magnetization do not alter the Debye temperature, the total entropy changes (in an isothermal process) is equal to the magnetic entropy change.

There are different ways to measure and calculate the adiabatic temperature change, ΔT_{ad}, that occurs for changes in the external magnetic field.[14] Our theoretical and experimental procedure was to determine the total entropy versus temperature curves at magnetic fields $H_1=0$ and $H_2=5$ T, from which the ΔT_{ad} was obtained using the equation

$$-\Delta T_{\mathrm{ad}}(T,\Delta H) = T_1(T) - T_2(T). \quad (8)$$

This quantity, for a given pair of curves $S_T(T,H_1)$ and $S_T(T,H_2)$, is determined by the adiabatic process condition, $S_T(H_1,T_1)=S_T(H_2,T_2)$.

EXPERIMENT

In order to verify the theoretical predicted behavior of the magnetocaloric effect in $R\mathrm{Ni}_5$ we prepared polycrystalline samples (with R=Er, Gd, Ho, Dy, Nd, and Ce). The starting materials had purities of 99.9% for the R elements, and 99.99% for Ni. After weighing appropriate proportions of the elements, the samples were arc-melted several times in a high purity atmosphere, being turned between meltings for homogenization. The samples were characterized using x-ray diffraction with Cu Kα radiation, which confirmed their single phase nature. Magnetic characterizations—Curie temperatures and saturation magnetization (where applicable)—were done in a commercial SQUID magnetometer in fields up to 7 T. The heat capacity was measured by the two tau method in a commercial relaxation calorimeter (PPMS from Quantum Design) without and with applied magnetic field of 5 T.

RESULTS AND DISCUSSIONS

In Table I we collected, for each compound of the $R\mathrm{Ni}_5$ series, all the necessary magnetic parameters to be used in our model presented above. The CEF parameters are in meV units and the exchange parameters are in T^2/meV. The eighth column gives the crystallographic directions of the easy magnetic direction which fixes the magnetic Hamiltonian, relation (3). For example, $HoNi_5$ has the *a*-crystalline easy axis, therefore, the proper direction cosines are $\cos(\alpha)=1$, $\cos(\beta)=0$, and $\cos(\gamma)=0$. It is worth noticing that since the magnetization variation, for materials with CEF anisotropy, generally depend on the applied magnetic field direction, so the magnetic entropy change is also dependent

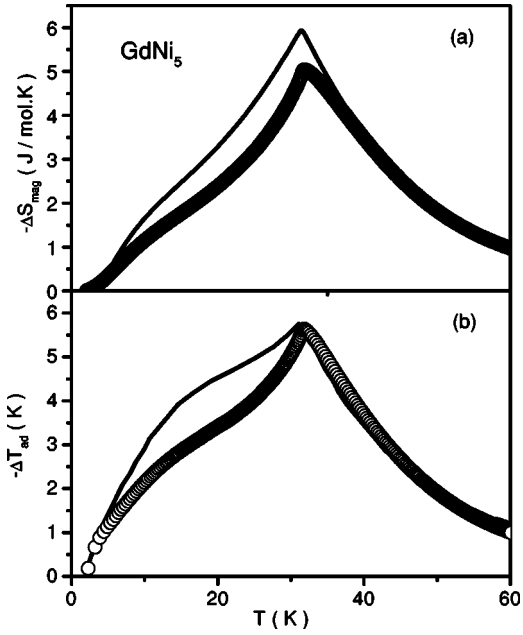

FIG. 1. Temperature dependence of ΔS_{mag} (a) and ΔT_{ad} (b) in GdNi_5 for a magnetic field change from 0 to 5 T. The solid lines represent the theoretical results and the open circles show the experimental data.

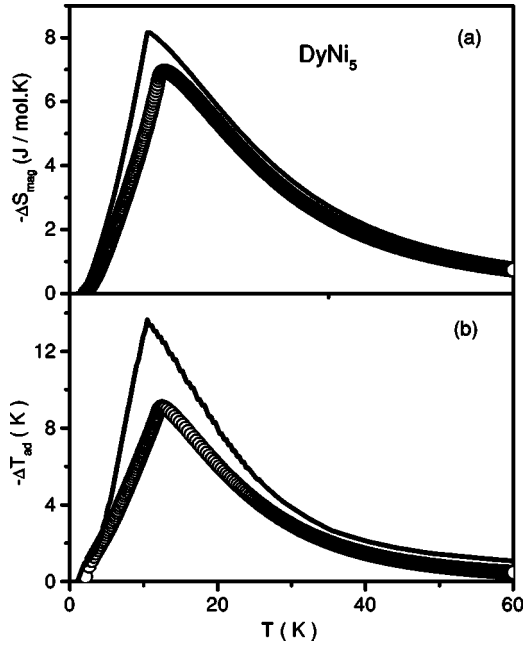

FIG. 2. Temperature dependence of ΔS_{mag} (a) and ΔT_{ad} (b) in DyNi_5 for a magnetic field change from 0 to 5 T. The solid lines represent the theoretical results and the open circles show the experimental data.

on the applied field direction in crystallographic axes. The theoretical calculations were performed in single-crystal assumption above discussed. The last column in Table I ives the references from where the parameters were obtained.

The lattice entropy of each compound of the $R\mathrm{Ni}_5$ series was estimated considering the isostructural and nonmagnetic compound LaNi_5. The temperature dependence of the Debye temperature in LaNi_5 was determined considering the Debye analytical expression for heat capacity and the tabulated experimental data for heat capacity versus temperature from Ref. 22. The adjustment was performed using a seventh order degree polynomial, i.e., $T_D(T)=\Sigma_{n=0}^{7} a_n T^n$. Therefore, the lattice entropy, relation (6), was determined at each temperature using the appropriate Debye temperature. It is worth noticing that, without this procedure, the calculation of the ΔT_{ad} vs T could not be obtained with the desirable numerical precision (necessary to guarantee the adiabatic process).

In Fig. 1 is displayed the ΔS_{mag} and ΔT_{ad} versus temperature in the GdNi_5 compound, calculated (solid line) and measured (open circles), for a magnetic field change from 0 to 5 T. The ΔS_{mag} and ΔT_{ad} maximum values occur at the Curie temperature, as expected, since at this temperature an applied magnetic field has maximum reduction effect on magnetic entropy for normal ferromagnetic systems. Since Gd is an S-state ion, the CEF parameters are neglected in the calculations. So the only magnetic parameter for this compound is the exchange parameter, which was determined to be $\lambda=38.39\ \mathrm{T}^2$ meV in order to fix the experimental Curie temperature from Ref. 13.

Figure 2 shows the ΔS_{mag} and ΔT_{ad} versus temperature, for a magnetic field change from 0 to 5 T for the DyNi_5 compound. Note that sharp peaks appear in the experimental data at the Curie temperature, for both curves, in accordance with the theoretical results. On the other hand, for HoNi_5, the theoretical calculation predicts broad peaks for ΔS_{mag} and ΔT_{ad} around the phase transition temperature, see Fig. 3, which are in good agreement with the experimental data.

For NdNi_5, the model parameters considered from Ref. 16, when used into the magnetic state equation, relation (4),

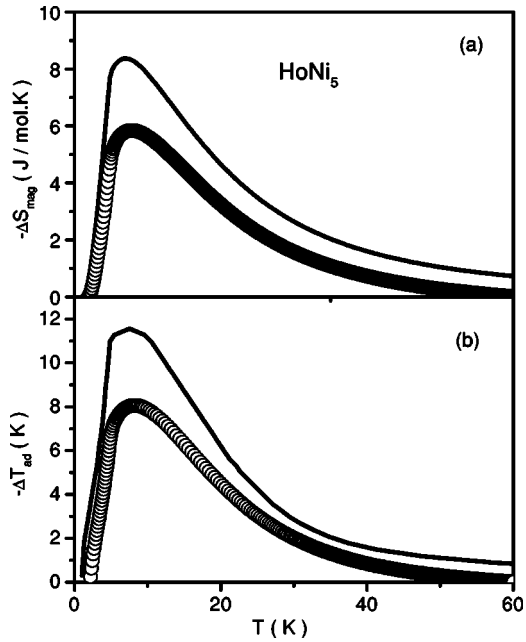

FIG. 3. Temperature dependence of ΔS_{mag} (a) and ΔT_{ad} (b) in HoNi_5 for a magnetic field change from 0 to 5 T. The solid lines represent the theoretical results and the open circles show the experimental data.

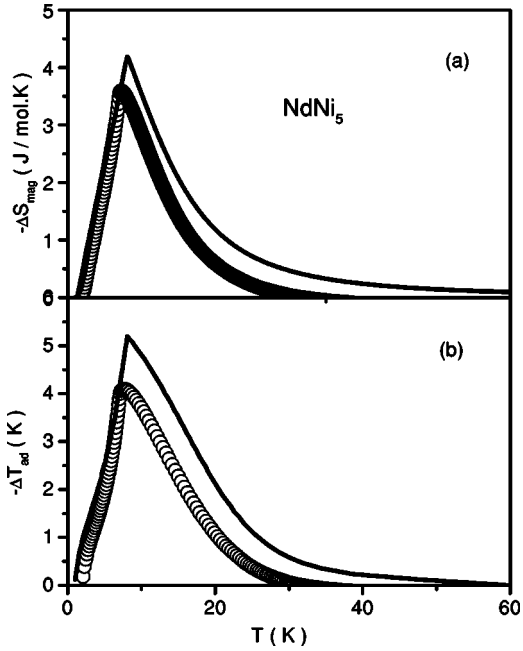

FIG. 4. Temperature dependence of ΔS_{mag} (a) and ΔT_{ad} (b) in $NdNi_5$ for a magnetic field change from 0 to 5 T. The solid lines represent the theoretical results and the open circles show the experimental data.

do not reproduce our experimental Curie temperature, as shown in Fig. 4. However, the theoretical curves present the same profile as the experimental ones.

For $TbNi_5$, as displayed in Fig. 5, again the magnetic parameters found in the literature provide good agreement between the theoretical curves and the experimental data for

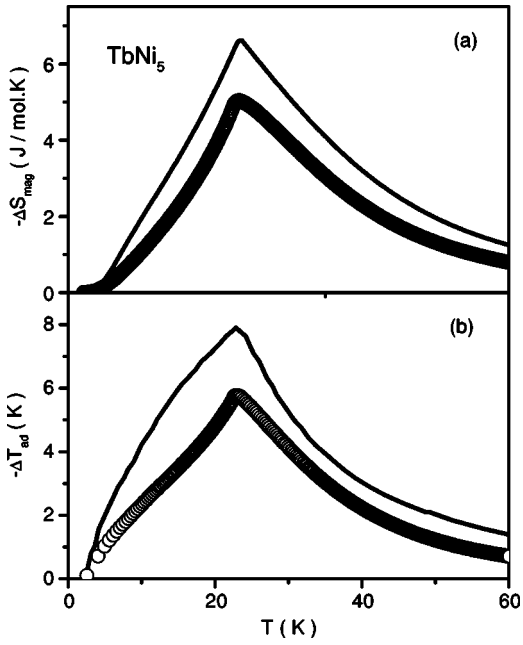

FIG. 5. Temperature dependence of ΔS_{mag} (a) and ΔT_{ad} (b) in $TbNi_5$ for a magnetic field change from 0 to 5 T. The solid lines represent the theoretical results and the open circles show the experimental data.

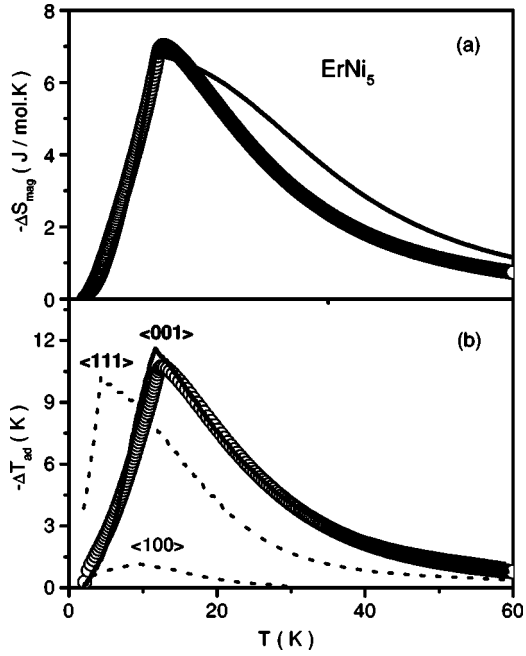

FIG. 6. Temperature dependence of ΔS_{mag} (a) and ΔT_{ad} (b) in $ErNi_5$ for a magnetic field change from 0 to 5 T. The solid lines represent the theoretical results and the open circles show the experimental data.

the magnetocaloric effect. In the ferromagnetic phase the concavity is positive for the ΔS_{mag} curve and negative for ΔT_{ad} curve versus temperature, showing the sensibility of the proper use of the CEF parameters. When we have low concentration (density of states) of magnetic levels in low temperature region, low magnetic entropy appears and therefore a negative concavity in ΔS_{mag} versus T is expected. The CEF controls the number of magnetic states at low temperature, and in general, the CEF interaction splits the $(2J+1)$-degenerated magnetic states.

Figure 6 shows the ΔS_{mag} and ΔT_{ad} versus T for $ErNi_5$. In this compound we found the best agreement between theory and experiment for the magnetocaloric effect [see Fig. 6(b)]. Note (see Table I) that the easy magnetic direction in $ErNi_5$ is perpendicular to the basal plane, i.e., it is in the c-crystallographic direction. In order to show the sensibility of the magnetocaloric effect on the change of direction of applied magnetic field we choose two other directions, namely $\langle 100\rangle$ (a direction in basal plane) and $\langle 111\rangle$ (diagonal cubic direction), see the dotted curves in Fig. 6(b). In the hard magnetization direction, the lowest ΔT_{ad} is obtained from the magnetic material for the same magnetic field change, in our case $\Delta H=5$ T. In addition, for the intermediate direction $\langle 111\rangle$, between the easy and hard magnetic directions, the model predicts a shift of about 7 K to below the Curie temperature in the ΔT_{ad} peak. This shift can be important in designing new refrigerant magnetic material. Nevertheless, experimental results using single crystals are necessary to confirm the predicted temperature shift.

Figure 7(a) presents the results for ΔS_{mag} versus T for the $PrNi_5$ compound. The theoretical model predicts an anomalous behavior in the entropy change below $T=14$ K in which the $PrNi_5$ (paramagnetic material) increases entropy when

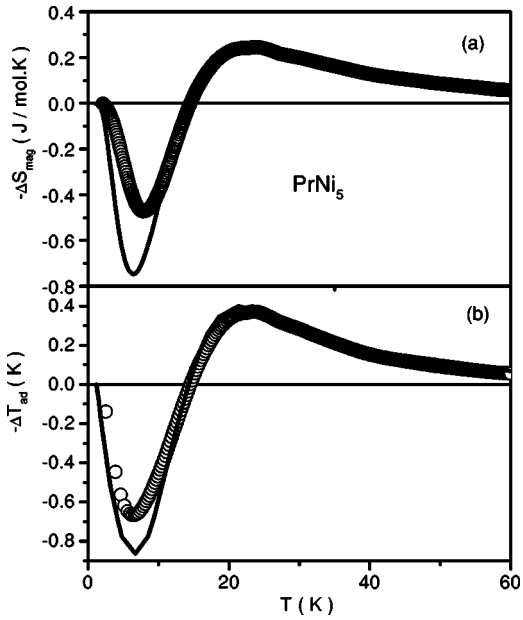

FIG. 7. Temperature dependence of ΔS_{mag} (a) and ΔT_{ad} (b) in PrNi_5 for a magnetic field change from 0 to 5 T. The solid lines represent the theoretical results and the open circles show the experimental data.

the magnetic field is applied. The origin of this anomaly was attributed to the crossing of the two fundamental CEF levels.[10] Nevertheless, as far as we know, the magnetocaloric effect, i.e., ΔT_{ad} versus T [see Fig. 7(b)] was not investigated in this compound. The anomalous MCE was theoretically predicted and measured quantitatively, i.e., the PrNi_5 compound cools upon magnetization and warm upon demagnetization below T=14 K. In fact, this result could be qualitatively expected from the thermodynamic relation that holds for the adiabatic process,

$$dT_{\mathrm{ad}} = -\frac{T}{C}\left(\frac{\partial S}{\partial H}\right)_T dH, \tag{9}$$

where C is the total heat capacity (a positive quantity). In the normal magnetic system, $\Delta S<0$ for $\Delta H>0$, leading to $\Delta T_{\mathrm{ad}}>0$. In our anomalous PrNi_5 case, for $\Delta H>0$ we get $\Delta S>0$ [see Fig. 7(a)] and therefore, from relation (9), $\Delta T_{\mathrm{ad}}<0$, as it was effectively determined from our specific heat measurements.

CONCLUSION

Using a model that includes CEF anisotropy we calculated the magnetocaloric thermodynamic quantities ΔS_{mag} and ΔT_{ad} versus temperature for the hexagonal magnetic systems, $R\mathrm{Ni}_5$ series, using the model parameters found in the literature for these compounds. Also, experimental work was performed in order to compare to our theoretical results. The agreement between theory and experiment for each compound is very satisfactory taken into account that no fitting procedure, adjusting model parameters, was performed. In general our theoretical curves for ΔS_{mag} and ΔT_{ad} reproduce our experimental results in profile but with slightly higher values than the experimental ones. This can be attributed to the fact that theoretical calculations were performed considering single crystals and the experiments were done using polycrystalline samples. The existence of the anomalous MCE (ΔT_{ad} vs T) in PrNi_5 was calculated and experimentally verified, with very good agreement. The anisotropy of the MCE in ErNi_5 was theoretically investigated applying the field into three different directions. As expected, the highest MCE occurs in the easy magnetic direction. The possibility change of the peak position of ΔT_{ad} vs T, in ErNi_5, when the applied field is considered in the $\langle 111\rangle$ direction, was theoretically predicted. This question requires further experimental investigation using single-crystalline samples.

ACKNOWLEDGMENTS

The authors acknowledge financial support from CNPq—Conselho Nacional de Desenvolvimento Científico e Tecnológico—Brazil, and from FAPESP—Fundação de Amparo à Pesquisa do Estado de São Paulo. This work was partially supported by PRONEX number E-26/171.168/2003 from FAPERJ/CNPq. One of us (P.J.v.R.) is grateful to Dr. Vitória M.T.S Barthem for fruitful discussion.

*Electronic address: vonranke@nitnet.com.br

[1] V. K. Pecharsky and K. A. Gschneidner, Jr., Phys. Rev. Lett. **78**, 4494 (1997).
[2] K. A. Gschneidner Jr., and V. K. Pecharsky, in *Rare Earths: Science, Technology and Application III*, edited by R. C. Bautista, C. O. Bounds, T. W. Ellis, and B. T. Kilbourn (The Minerals, Metals and Materials Society, Warendale, PA 1997).
[3] O. Tegus, E. Bruck, K. H. J. Buschow, and F. R. de Boer, Nature (London) **415**, 150 (2002).
[4] H. Wada and Y. Tanabe, Appl. Phys. Lett. **79**, 20 (2001); **79**, 3302 (2001).
[5] H. Wada, T. Morikawa, K. Taniguchi, T. Shibata, Y. Yamada, and Y. Akishige, Physica B **328**, 114 (2003).
[6] P. J. von Ranke, N. A. de Oliveira, and S. Gama, J. Magn. Magn. Mater. **277**, 78 (2004).
[7] P. J. von Ranke, A. de Campos, L. Caron, A. A. Coelho, S. Gama, and N. A. de Oliveira (unpublished).
[8] P. J. von Ranke, N. A. de Oliveira, and S. Gama, Phys. Lett. A **320**, 302 (2004).
[9] P. J. von Ranke, A. L. Lima, E. P. Nóbrega, X. da Silva, A. P. Guimarães, and I. S. Oliveira. Phys. Rev. B **63**, 024422 (2001).
[10] P. J. von Ranke, V. K. Pecharsky, K. A. Gschneidner, and B.J. Korte., Phys. Rev. B **58**, 14 436 (1998).
[11] K. H. J. Buschow and A. S. van der Goot, Acta Crystallogr., Sect. B: Struct. Crystallogr. Cryst. Chem. **27**, 1085 (1971).
[12] K. W. H. Stevens, Proc. Phys. Soc., London, Sect. A **65**, 209 (1952).
[13] R. J. Radwanski, N. H. Kim-Ngan, F. E. Kayzel, J. J. M. Franse,

D. Gignoux, D. Schmitt, and F. Y. Zhang, J. Phys.: Condens. Matter **4**, 8853 (1992).
[14] A. M. Tishin, "Magnetocaloric effect in the vicinity of phase transitions," in *Handbook of Magnetic Materials*, edited by K. H. J. Buschow (North-Holland Elsevier, Amsterdam, the Netherlands, 1999), Vol. 12, Chap. 4, pp. 395–524.
[15] N. Marzouk, R. S. Graig, and W. E. Wallace, J. Phys. Chem. Solids **34**, 15 (1973).
[16] V. M. T. S. Barthem, D. Gignoux, and D. Schmitt, J. Magn. Magn. Mater. **78**, 56 (1989).
[17] F. Y. Zhang, D. Gignoux, D. Schmitt, J. J. M. Franse, F. E. Kayzel, N. H. Kim-Ngan, and R. J. Radwanski, J. Magn. Magn. Mater. **130**, 108 (1994).
[18] L. Morellon, P.A. Algarabel, M. R. Ibarra, A. del Moral, D. Gignoux, and D. Schmitt, J. Magn. Magn. Mater. **153**, 17 (1996).
[19] V. M. T. S. Barthem, D. Gignoux, A. nait-Saada, D. Schmitt, and A. Y. Takeuchi, J. Magn. Magn. Mater. **80**, 142 (1989).
[20] D. Gignoux, D. Givord, and A. del Moral, Solid State Commun. **19**, 891 (1976).
[21] A. Andreeff, V. Valter, H. Grissmann, L. P. Kaun, B. Lipold, V. Mats, and T. Franzkhaim, JINR Rapid Commun. **1978**, P14–11324 (1978).
[22] N. Marzouk, R. S. Graig, and W. E. Wallace, J. Phys. Chem. Solids **34**, 15 (1973).